

DYNAMIC IDENTIFICATION OF A RECTANGULAR FOUNDATION RAFT ON PILES

G. BUDA¹, G. OLIVETO¹

¹Department of Civil and Environmental Engineering, Structural Engineering Division, University of Catania, Catania, Italy. < gbuda@dica.unict.it, golive@dica.unict.it >.

ABSTRACT

This paper presents a first attempt at the dynamic identification of a soil-structure interacting system. After the description of the structure, a foundation raft on piles, and of the experimental equipment used, a modern procedure for the identification of the modal parameters is applied. The experimental modal shapes display some asymmetries not predictable on the basis of the geometry and mechanical characteristics of the structural system. These asymmetries find acceptable physical explanations from the additional restraints imposed by local contact with adjacent structures. The construction and updating of a numerical model has lead to the reliable evaluation of some, but not all, of the soil-pile dynamic stiffnesses. For the remaining ones it is felt that the evaluated real part is sufficiently accurate while a considerable uncertainty remains concerning the imaginary part.

1. INTRODUCTION

In the evaluation of the response of engineering structures to earthquakes, a significant role is often played by soil-structure interaction. In order to account for the dynamic soil-structure interaction adequate models are required for the structure, for the foundation and for the soil. The situation becomes rather complex for foundations on piles where the interface between a foundation and the soil is quite extensive. From the point of view of the structural engineer or of the earthquake engineer a proper model of the soil-foundation system is of great importance for the prediction of the seismic response of the soil-structure interactive system.

Reliable models of the soil-foundation system may be constructed by using boundary element method procedures or coupled boundary element-finite element method procedures. Simplified models for the dynamic soil-pile system have been presented in the literature mainly based on the work by Novak [1, 2]. However the reliability of the numerical and simplified models is difficult to ascertain especially because of the great variability of the soil properties even within a confined region.

The main objective of the present work is to provide an experimental evaluation of the dynamical characteristics of the foundation-soil system for use in the calibration of numerical and simplified models. To this purpose a rectangular foundation raft on piles is considered. This particular raft has been subject to static and dynamic load tests. The latter were of an

impulsive and of a harmonic type. However in this work only the dynamic harmonic tests will be presented, discussed and used.

A secondary objective of the present work is the calibration of a numerical model that reproduces quite closely the observed experimental behaviour and provides good estimates of the dynamical characteristics of the soil-foundation systems.

A fallout of this application will be the evaluation of the mechanical characteristics of a simplified soil-pile model.

2. THE FOUNDATION SYSTEM

A foundation raft on piles, that was built as part of the supplemental foundation in the seismic retrofitting of a reinforced concrete building damaged by a moderate earthquake on December 13th 1990 in south-east Sicily, has been selected for the experimental tests.

The raft is built on 18 reinforced concrete piles driven in clayey soil. The diameter of the 30 m long piles is 50 cm and the disposition in plan is represented in Fig. 1. The size of the reinforced concrete raft is 11.80 m x 3.20 m x 1.00 m.

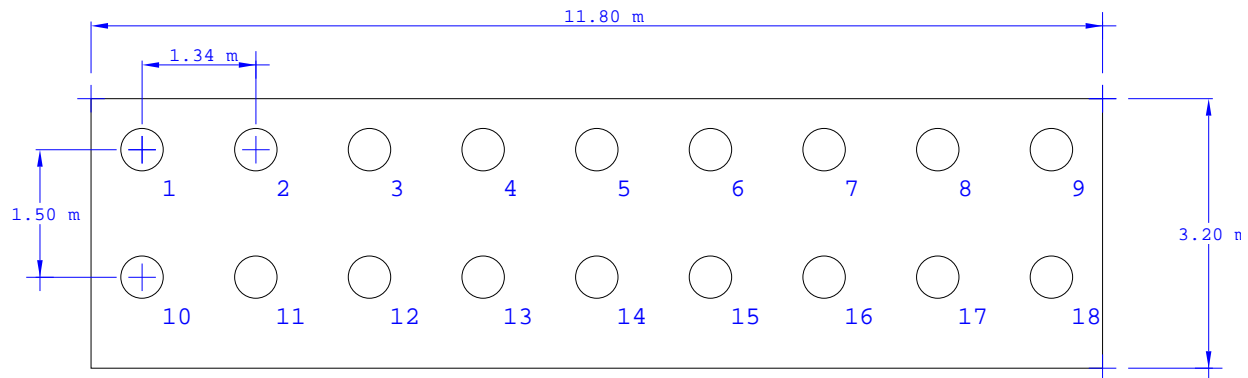


Figure 1. Raft geometry and piles layout.

The piles were reinforced with 10 steel bars of 24 mm diameter for the upper 11 metres and with 10 steel bars of 18 mm diameter for the remaining 19 metres. There is also a 8 mm diameter helical reinforcement with a step of 8 cm for the first 11 metres and 12 cm for remaining 19 metres. All piles were subject to cross-hole sonic integrity tests.

3. GEOLOGICAL AND GEOTECHNICAL CONDITIONS

A brief summary of the geological and geotechnical conditions at the site is reported in reference [3]. Here it suffices to know that the piles are driven into soft soil of variable characteristics up to a depth of 15 metres after which the characteristics become roughly constant. The longitudinal and shear wave velocities evaluated up to a depth of 80 metres, show a roughly parabolic increase from the surface down to 15 metres and then remain constant ($V_l=1800$ m/s, $V_s=600$ m/s). Apart from the initial 15 metres the foundation soil is a thick layer of grey-blue infra-pleistocene clay which may reach depths of the order of 300-500 metres. Because of the strong variability of the soil properties for more than half of the pile length it has been considered appropriate to use a simplified model for the soil-pile system.

4. EXPERIMENTAL EQUIPMENT

The excitation has been provided by a harmonic actuator in the frequency range 5-15 Hz. The applied harmonic load has been measured by means of specifically designed load cells and acquired by a suitable dynamic data acquisition system. Therefore all the characteristics of the applied load have been clearly evaluated. The amplitude of the applied load varied from a minimum of 6 kN at 5 Hz to a maximum of 50 kN at 15 Hz.

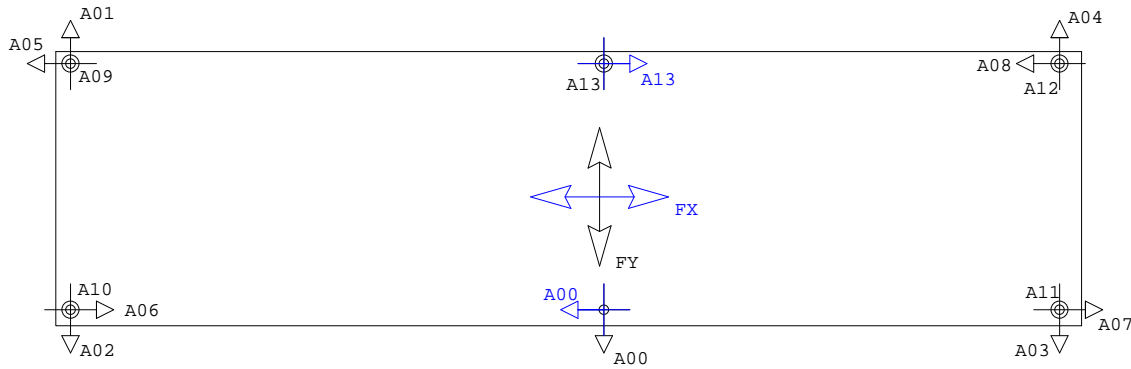


Figure 2. Experimental set-up.

The response of the structural system has been measured by means of 14 piezoelectric acceleration transducers with the following characteristics: resolution 10^{-6} g, amplitude range ± 0.5 g, sensitivity 10 V/g. The accelerometers were disposed, as shown in Fig. 2, in a three-axial configuration at each of the four corners on the roof of the raft and the remaining two in a mono-axial configuration along one of the axes of symmetry of the raft. These two accelerometers were oriented along the direction where the test was performed, that is in a longitudinal or transverse direction according to the case.

4.1. Data acquisition

The response was acquired by means of a suitable dynamic data acquisition system. The frequency response functions (FRF) were evaluated at all the measurement points for each of the measured acceleration components. The frequency step used in the experimental test and in the construction of the FRF was equal to 0.1 Hz. At each step the response was recorded for 90 seconds after the transient phase had expired. The sampling frequency was set at 100 Hz and considered sufficiently high in view of the frequency range of interest. Obviously the same procedure was used for the acquisition of the exciting force. The analogue signals produced by the accelerometers and the load cells are properly conditioned before being fed into the analogue-to-digital converter and then recorded and stored in ASCII format.

5. IDENTIFICATION OF MODAL PARAMETERS

The frequency response functions (inertances) were constructed from the recorded signals for each recorded acceleration signal. Therefore, for each testing direction, 14 FRF were constructed. Four FRF are shown in Fig. 3a for the test in the transverse direction, and in Fig. 3b for the test in the longitudinal direction. The representation is given both in terms of amplitude and phase and in terms of real and imaginary parts.

The acceleration signals considered refer both to the direction of testing and to the measurement points at the four corners of the raft.

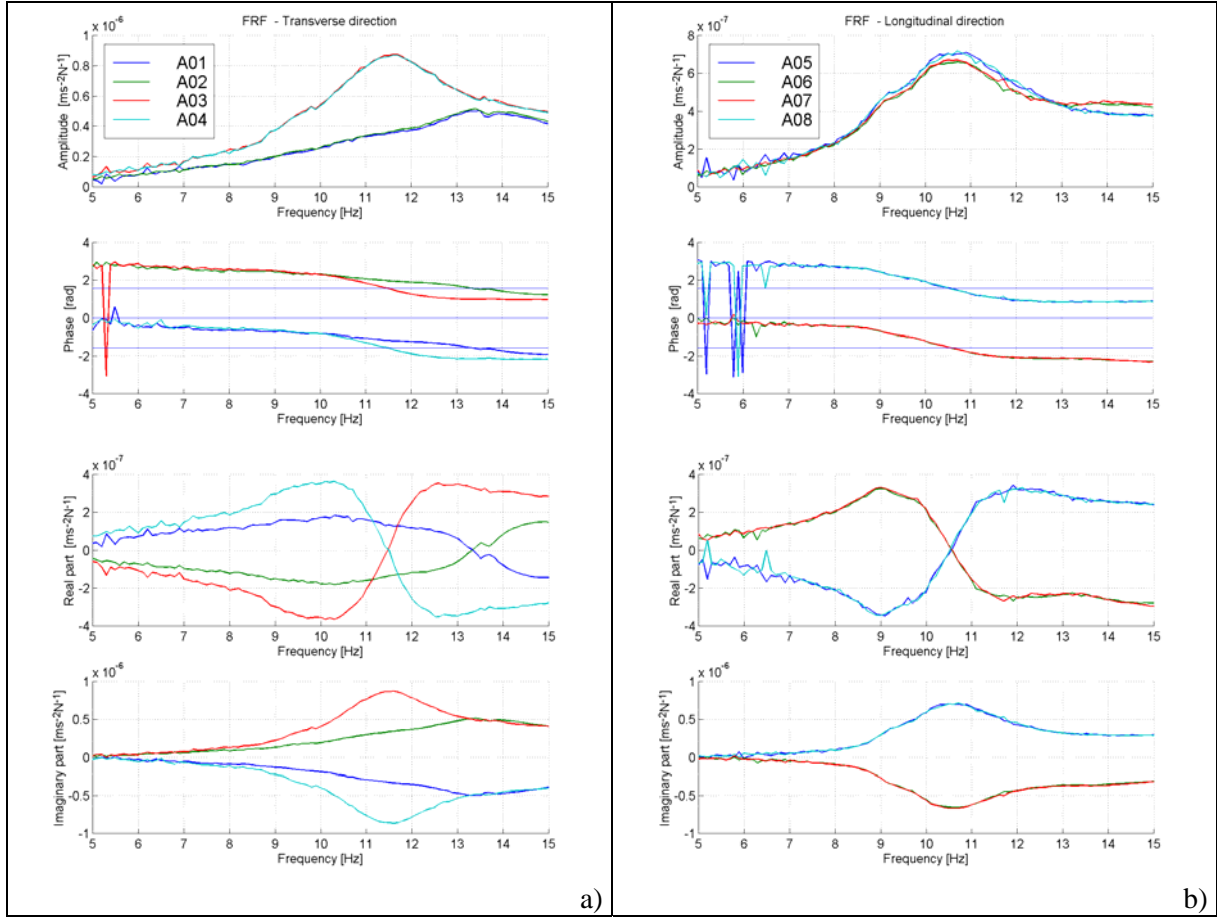


Figure 3. a) FRF for the test in the transverse direction;
b) FRF for the test in the longitudinal direction.

5.1. Identification of the modal parameters

The FRF generated have been used to estimate poles and residues from which frequencies, damping ratios and modal shapes may be derived. The IDRC algorithm [4] has been used to estimate poles and residues while the IDRМ algorithm [4, 5] has been used for consistency checks on these results and to derive frequencies, damping ratios and modal shapes. In the investigated frequency range three modes have been identified. The poles, frequencies and damping ratios identified are shown in Table 1, while the corresponding modal shapes are represented in Fig. 4. Each modal shape is shown in plan and in a three-dimensional view.

Table 1 Identified modal parameters: pole λ , natural frequency ω , damped frequency ω_D , damping ratio ξ .

Mode	λ [Hz]	ω [Hz]	ω_D [Hz]	ξ [%]
1	$-1.5425 - i 10.106$	10.2230	10.1060	15.088
	$-1.5425 + i 10.106$			
2	$-1.3027 - i 11.734$	11.8060	11.7340	11.034
	$-1.3027 + i 11.734$			
3	$-3.3455 - i 12.669$	13.1032	12.6690	25.532
	$-3.3455 + i 12.669$			

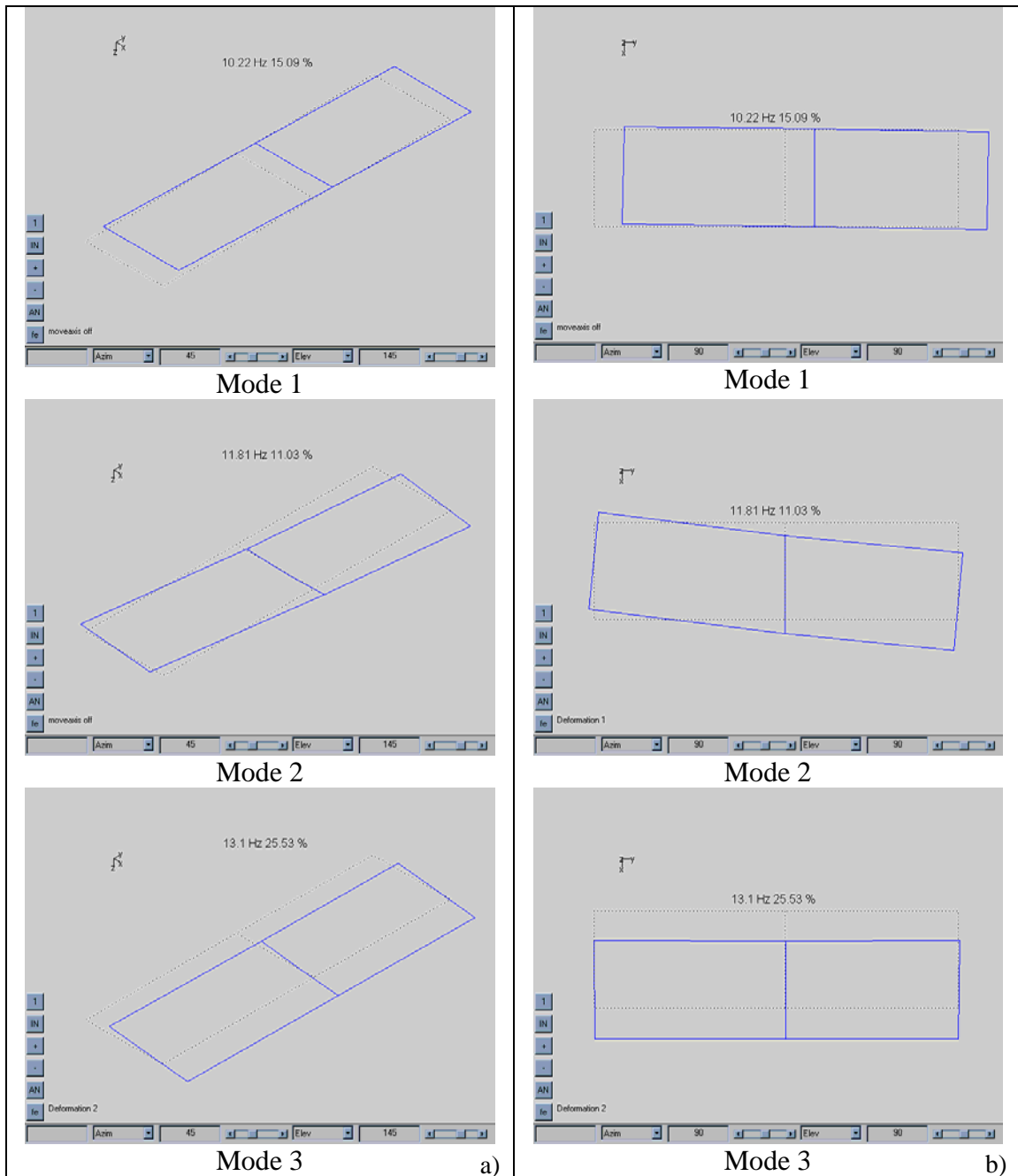


Figure 4. Identified modal shape: a) three dimensional view, b) plan view.

From the observation of the modal shapes it is possible to conclude that the first mode, corresponding to a natural frequency of 10.22 Hz, is translatory in the longitudinal direction. The second mode, corresponding to a natural frequency of 11.81 Hz, appears to be a coupled translatory and rotational motion. The translation occurs in the transversal direction while the rotation occurs in the horizontal plane.

The third mode, corresponding to a natural frequency of 13.10 Hz, is also a coupled translatory and rotational mode. This time the coupling is weaker and the rotation occurs in the vertical plane.

Given the geometrical and mechanical symmetry of the structure with respect to the transverse axis, one would have expected a symmetric translatory mode in the transverse

direction and a pure torsional mode. Some weak coupling could have been also expected, but the predominance of the translatory motion, in one case, and of the rotational motion, in the other case, should have been evident.

The third mode seems, in fact, to fall in this class. However the strong coupling present in the second mode points to the existence of some sort of asymmetry in the system. The presence of this asymmetry renders the present problem more rewarding and the calibration of numerical models more challenging.

6. NUMERICAL MODEL UPDATING

A numerical model of the raft-soil-piles system has been formulated by using solid finite elements for the raft and linear spring elements for the soil-pile system. Each soil-pile system has been idealised by three independent linear springs along three perpendicular axes one of which being coincident with the pile axis and the other two being parallel to the axes of the raft. The mass density and the mechanical properties of the raft have been considered to be known. Therefore the main object of the numerical model updating has been a reliable estimate of the stiffness of the linear springs. Overall a total of 54 stiffnesses (3 stiffnesses/pile \times 18 piles = 54 stiffnesses) need to be estimated.

6.1. Updating procedure

The updating procedure of the numerical model is based on the constrained least squares minimisation of the relative error between the numerical and experimental values of the first three frequencies. As in any numerical optimisation procedure a starting point is needed. In this case the initial spring stiffnesses were evaluated on the bases of the simplified model by Novak [1]. Due to the variability of the soil properties with depth, average values were used. In particular the following values were used for the longitudinal, transverse and vertical stiffnesses: $K_l = 25881 \text{ kNm}^{-1}$, $K_t = 34508 \text{ kNm}^{-1}$, $K_v = 447036 \text{ kNm}^{-1}$.

The constraints are applied by setting lower and upper bounds for each spring stiffness on the basis of physical expectation. The lower bound for each type of spring stiffness was set equal to 24000 kNm^{-1} while the upper bound was set equal to 480000 kNm^{-1} .

From the starting point the least squares optimisation procedure is applied to reach a new state or point. The procedure is iterated until the final state differs from the previous one by less than a prescribed tolerance. The control parameter for the tolerance is the mean-square error calculated from the three considered frequencies.

6.2. Optimal model reliability

The optimal model obtained for a prescribed tolerance $\varepsilon = 0.001$ after 7 iterations has been subjected to assurance tests in order to ascertain the degree of correlation with the actual structure as described by the experimental data.

A comparison of the experimental and numerical frequencies is given in Table 2 for the start-up model and for the optimal one. As may be seen from the table, the error in the individual frequencies is less than 1%, actually only one or two units in a thousand. The same error for the start-up model is considerably higher.

The modal assurance coefficients (MAC), that provide the degree of correlation between the experimental and numerical modal shapes, are also given in Table 2 for the start-up and for the optimal model. It may be of interest to notice that the MAC coefficients for the first two modal shapes are quite close to one already for the start-up model, indicating a good correlation with the experimental modal shapes. However the MAC coefficient for the third

mode is nearly zero, indicating lack of correlation between the experimental and numerical modal shapes. The cross correlation coefficients, that should be zero for a good correlation between experimental and numerical modal shapes, are not given in the table but are quite large with reference to the third mode, as may be inferred from the histogram of Fig. 5.

Table 2. Experimental and numerical frequencies, relative error and MAC coefficients.

Mode	Experimental frequency	Start-up model			Optimal model		
	[Hz]	[Hz]	Error [%]	MAC	[Hz]	Error [%]	MAC
1	10.2232	10.2618	0.40	0.92	10.2252	0.02	0.95
2	11.6147	11.6392	0.20	0.79	11.6321	0.15	0.97
3	13.3190	11.8374	-11.10	0.02	13.3210	0.01	0.36
		Root mean square error : 11.95 %			Root mean square error : 0.09 %		

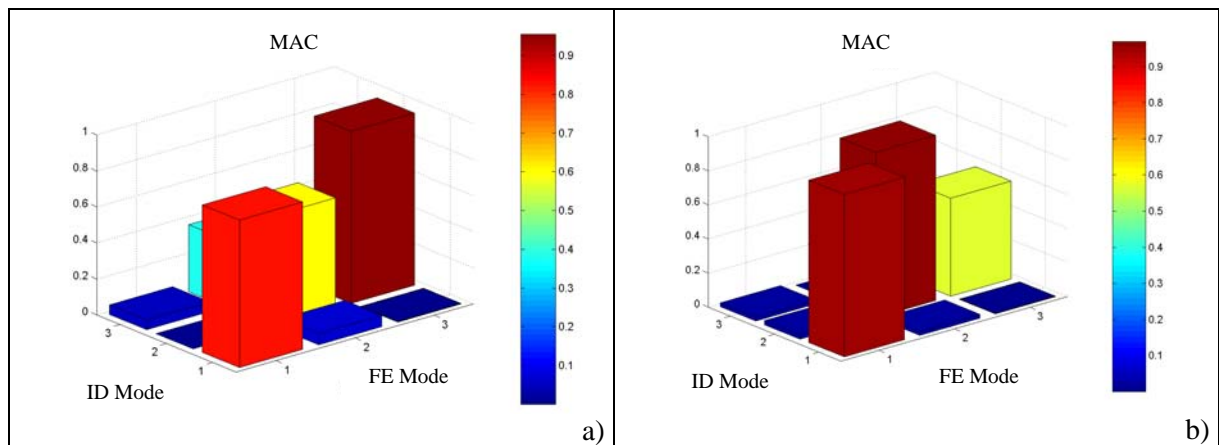


Figure 5. a) MAC coefficient between start-up model and experimental model: b) MAC coefficient between optimal model and experimental model.

The direct MAC coefficients for the optimal solution are improved considerably with the respect to those for the start-up model. However the MAC coefficient for the third mode is still relatively low and much smaller than one of the cross coefficients, as may be gathered from the histogram of Fig. 5b.

This analysis shows that the final updated model describes quite well the frequency characteristics of the real system and sufficiently well the first two modal shapes, while the third one appears to be still a poor approximation. The reason for this behaviour may come from the fact that the actual modal shapes may be complex, rather than real, and the model adopted here might not be suitable for the description of the real structure.

A further check on the reliability of the updated model can be done on the FRF. The check is known by the acronym of FRAC (Frequency Response Assurance Criterion) [6] and provides a measure of the distance between the experimental and numerical FRF. A FRAC coefficient of one indicates perfect correlation between numerical and experimental FRF while a zero value indicates independent FRF. In the present work the FRAC coefficients have been evaluated for all the available experimental FRF and corresponding numerical ones. The results are shown in Fig. 6a for the test in the longitudinal direction and in Fig. 6b for the test in the transverse direction. In the same figure are shown also the corresponding FRAC coefficients for the start-up model. It may be worth noticing that the FRAC

coefficients for the relevant degrees of freedom (response parameter in the same directions as the excitation) are all very close to one, indicating a good correlation between the experimental and numerical FRF. However the FRAC coefficients for the non-relevant degrees of freedom may be in some cases rather low indicating a poor correlation for the considered FRF.

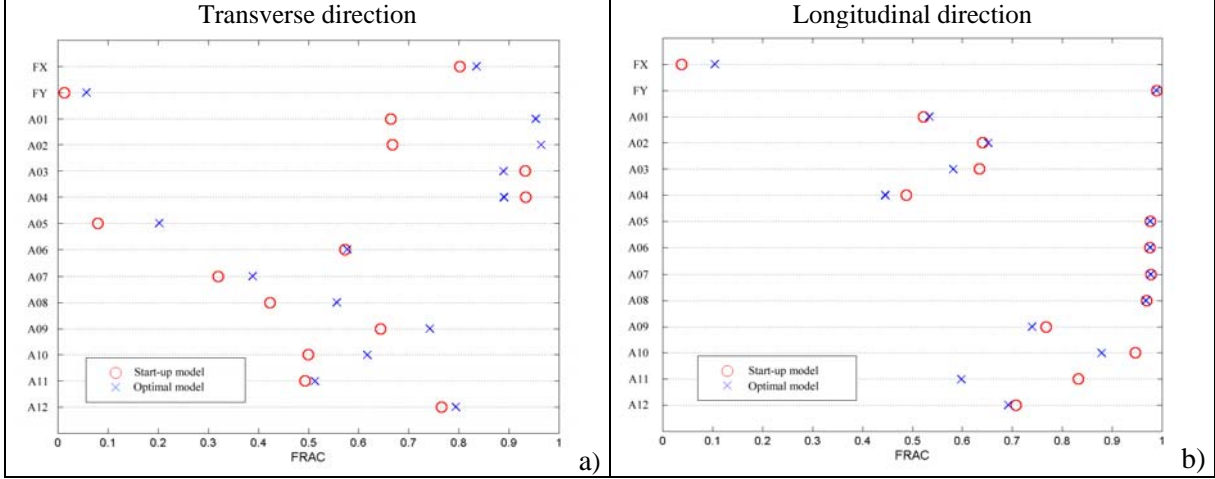


Figure 6. FRAC coefficient: a) test in transverse direction, b) test in the longitudinal direction.

6.3. Soil-pile stiffnesses

The asymmetry displayed by the experimental model and by the optimal numerical model derives from the distribution of the stiffnesses of the soil-pile systems. The optimal model provided the following values for the stiffnesses of the soil-pile systems: $K_t=25496 \text{ kNm}^{-1}$, $K_t=34123 \text{ kNm}^{-1}$ and $K_v=446651 \text{ kNm}^{-1}$ for all piles apart from pile 10, Fig.1, which exhibits a considerably larger transversal stiffness, $K_t=92483 \text{ kNm}^{-1}$. This values is nearly four times larger than the corresponding value for the other piles. A physical explanation of this behaviour may not be found in differences in the soil or in the pile but rather in some additional restraint on the transverse motion provided by a possible local contact between the pile considered and a pile of the existing foundation due to imperfect construction. This could explain the additional stiffness that would be provided by the existing foundation.

7. DIRECT MODAL DAMPING IDENTIFICATION

The observation of the modal shapes shows that the contribution of the second and third mode to the FRF to longitudinal degrees of freedom is negligible. By neglecting also the contribution of higher modes, the first mode dynamical characteristics may be identified directly from the FRF corresponding to the longitudinal degrees of freedom.

The first mode equation of motion may be written as follows (Equation 1):

$$\left[K_1 - \omega^2 M_1 + i\omega C_1 \right] u_1(\omega) = f(\omega) \quad (1)$$

where M_1 , C_1 and K_1 are respectively the modal mass, the modal damping coefficient and the modal stiffness, while $f(\omega)$ is the amplitude of the harmonic excitation. The complex dynamic stiffness function may be derived directly from Equation 1:

$$\mathbf{K}_1 - \omega^2 \mathbf{M}_1 + i\omega \mathbf{C}_1 = \frac{\mathbf{f}(\omega)}{\mathbf{u}_1(\omega)} \quad (2)$$

The first mode displacement $u_1(\omega)$ may be assimilated into any one of the longitudinal degrees of freedom. There are 6 experimental longitudinal degrees of freedom and each one of them gives rise to an experimental dynamic stiffness function. A curve fitting procedure provides the first mode characteristics given in Table 3.

Table 3. First mode characteristics.

FRF	Modal mass M_1 [Ns^2m^{-1}]	Modal stiffness K_1 [Nm^{-1}]	ω_l [Hz]	Modal damping C_1 [Nsm^{-1}]	ξ_l
A05	110113.35	502537051.63	10.752	3196519.39	0.215
A06	101430.30	482162427.53	10.973	3337758.28	0.239
A00	102074.63	488487694.11	11.010	3389808.66	0.240
A07	102646.20	457235860.70	10.622	3320616.07	0.242
A08	99118.75	473115232.04	10.996	3289397.13	0.240
A13	108564.01	493942040.05	10.735	3354681.65	0.229
m	103991.21	482913384.34	10.848	3314796.86	0.234
σ_m	3961.745	14683865.516	0.151	61119.232	0.010
c.o.v. [%]	3.810	3.041	1.391	1.844	4.113

The curve fitting procedure is displayed in Fig. 7 with reference to the A05 dynamic stiffness function. It should be noticed that while the fitting is rather good for the real part of the dynamic stiffness function, it is only an average approximation for the imaginary part that provides damping. This might explain the difference in the predicted damping ratio (23.4%) with respect to the value obtained by the experimental identification (15.1%).

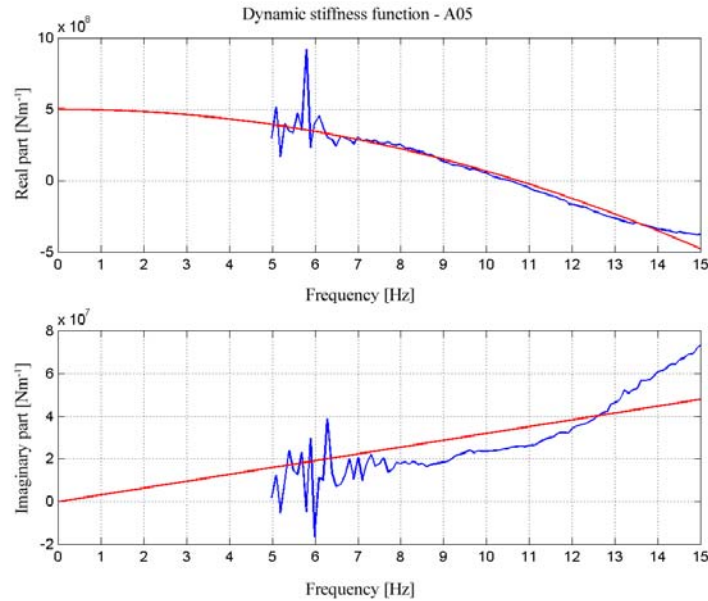


Figure 7. Dynamic stiffness function: a) real part, b) imaginary part.

Furthermore, from Fig. 7b, it appears that the modal damping coefficient cannot be considered frequency independent.

By considering that stiffness and damping are provided predominantly by the soil-pile systems and mass is provided predominantly by the raft, the following expressions Table 4 may be provided for the dynamic stiffness of the longitudinal soil-pile systems.

Table 4. Longitudinal dynamic stiffness of a soil-pile system.

	Model updating	FRF curve fitting
$K_1 + i \omega C_1$ [kNm ⁻¹]	25496 + i ω 120	26829 + i ω 184

The differences are due to the different degrees of approximation of the experimental data by the two identification procedures that have been used. The difference in the real parts is of the order of 5% and therefore well within engineering tolerances. The difference in the damping coefficient is more pronounced but may be attributed to the poor fitting in the second method.

8. CONCLUSION

Some procedures for the dynamic identification of a foundation raft on piles have been presented. The dynamic stiffness for the soil-pile system has been evaluated at least in the longitudinal direction. In the transverse and vertical directions the real parts can be considered as sufficiently accurate while the imaginary part, related to damping, is of a more problematic evaluation. The classical modal synthesis leads to not sufficiently accurate results because the actual modes are complex rather than real. Therefore this contribution must be viewed only as a first step towards the identification of soil-structure interacting systems. Further studies considering complex modal shapes and frequency dependent dynamic stiffnesses could lead to more reliable results.

9. REFERENCES

- [1] Novak M., El Sharnouby B., *Stiffness Constants of Single Piles*, Journal of Geotechnical Engineering, vol. 109 (7), July, 1983.
- [2] Novak M., *Pile-soil-pile interaction under small and large displacements*, Developments in Dynamic Soil-Structure Interaction, Kluwer Academic Publishers, pp. 361-380, 1993.
- [3] Oliveto G., Decanini L. D., *Repair and retrofit of a six storey reinforced concrete building damaged by the earthquake in South-east Sicily on the 13th December 1990*. Soil Dynamics and Earthquake Engineering, 17 (1), pp. 57-71, 1998.
- [4] Balmès E., *New results on the identification of normal modes from experimental complex modes*, Mechanical System and Signal Processing, 11-2, pp. 229-243, 1997.
- [5] Balmès E., *Integration of Existing Methods and User Knowledge in a MIMO identification algorithm for structures with high modal densities*, IMAC, pp 613-619, 1993.
- [6] Heylen W., Lammens S., Sas P., *Modal analysis theory and testing*, Katholieke Universiteit Leuven, Belgium, 1997.